GEOLOGY | THE GEOLOGICAL SOCIETY OF AMERICA®

https://doi.org/10.1130/G46837.1

Manuscript received 3 August 2019
Revised manuscript received 3 October 2019
Manuscript accepted 4 October 2019

Published online 19 November 2019

Biomediation of submarine sediment gravity flow dynamics

Melissa J. Craig[1], Jaco H. Baas[2], Kathryn J. Amos[1], Lorna J. Strachan[3], Andrew J. Manning[4], David M. Paterson[5], Julie A. Hope[6], Scott D. Nodder[7] and Megan L. Baker[2]

[1]Australian School of Petroleum, The University of Adelaide, Adelaide, South Australia 5000, Australia
[2]School of Ocean Sciences, Bangor University, Menai Bridge LL59 5AB, UK
[3]School of Environment, University of Auckland, Auckland 1142, New Zealand
[4]HR Wallingford, Howbery Park, Wallingford OX10 8BA, UK
[5]Scottish Oceans Institute, School of Biology, University of St. Andrews, St. Andrews KY16 8LB, UK
[6]Institute of Marine Science, University of Auckland, Auckland 1142, New Zealand
[7]National Institute of Water & Atmospheric Research, Wellington 6021, New Zealand

ABSTRACT

Sediment gravity flows are the primary process by which sediment and organic carbon are transported from the continental margin to the deep ocean. Up to 40% of the total marine organic carbon pool is represented by cohesive extracellular polymeric substances (EPS) produced by microorganisms. The effect of these polymers on sediment gravity flows has not been investigated, despite the economic and societal importance of these flows. We present the first EPS concentrations measured in deep-sea sediment, combined with novel laboratory data that offer insights into the modulation of the dynamics of clay-laden, physically cohesive sediment gravity flows by biological cohesion. We show that EPS can profoundly affect the character, evolution, and runout of sediment gravity flows and are as prevalent in deep oceans as in shallow seas. Transitional and laminar plug flows are more susceptible to EPS-induced changes in flow properties than turbulent flows. At relatively low concentrations, EPS markedly decrease the head velocity and runout distance of transitional flows. This biological cohesion is greater, per unit weight, than the physical cohesion of cohesive clay and may exert a stronger control on flow behavior. These results significantly improve our understanding of the effects of an unrealized biological component of sediment gravity flows. The implications are wide ranging and may influence predictive models of sediment gravity flows and advance our understanding about the ways in which these flows transport and bury organic carbon globally.

INTRODUCTION

Clay, inherently associated with organic matter, is the most abundant sediment type on Earth (Hillier, 1995). Recent advances in our understanding of the properties of clay have redefined our models of submarine sediment gravity flows (SGFs) in both modern and ancient environments (Wright and Friedrichs, 2006; Barker et al., 2008; Sumner et al., 2009). SGFs are volumetrically the most significant sediment transport process in the ocean, they can pose destructive hazards to offshore infrastructure, and their deposits form major hydrocarbon reservoirs (Talling, 2014). Understanding and prediction of SGF behavior therefore have scientific, economic, and social importance.

Clay-rich SGFs are governed by the ability of clay minerals to aggregate, or flocculate (McCave and Jones, 1988). Laboratory experiments of clay-rich SGFs show that at sufficiently high concentrations of clay, flocs bind to form a network that behaves as a gel, increasing viscosity and suppressing shear-generated turbulence (Baas and Best, 2002; Baas et al., 2009). These flows, and their deposits, are radically different to fully turbulent flows and highlight the importance of understanding how cohesive material affects SGFs.

Extracellular polymeric substances (EPS) are secreted by microorganisms in many environments, from rivers and estuaries to hypersaline systems and deep-sea hydrothermal vents (Decho and Gutierrez, 2017). The adhesion of this exopolymer to sediment grains forms a matrix of EPS, sediment, and single-cell organisms called a biofilm, which is considered to be the primary mechanism by which benthic microorganisms stabilize the sediment they inhabit (Tolhurst et al., 2002). Small concentrations of EPS (C_{EPS} < 0.063% by weight, wt%), representing baseline levels in estuarine sediment, can increase the development time of bed forms exponentially (Malarkey et al., 2015). EPS research to date has focused on coastal environments. The presence of EPS in deep-sea sediment and their impact on SGFs is not known.

EPS represent up to 40% of the marine organic carbon pool (Falkowski et al., 1998). The burial of organic carbon (C_{org}) in marine sediment represents the second largest sink of atmospheric CO_2 (Galy et al., 2007). However, global carbon budget studies typically estimate C_{org} flux by measuring the particulate organic matter settling through the water column and accumulating in marine sediment (Martin et al., 1987; Muller-Karger et al., 2005; Decho and Gutierrez, 2017). SGFs are not currently considered to be a significant C_{org} transport and burial process in C_{org} flux models on continental margins. This is surprising, since fine-grained sediment flows have been found to transport the majority of C_{org} (de Haas et al., 2002). Here, we present the first measurements of EPS from deep-sea sediment cores, and, through novel experiments, we test if EPS-derived biological cohesion is capable of inhibiting turbulence and intensifying cohesive SGF behavior. This has fundamental implications for (1) understanding SGF behavior in the natural environment, (2) models of C_{org} flux on continental margins and estimating C_{org} burial, as well as (3) reconstruction of past environments from ancient deposits and predicting hydrocarbon reservoir properties.

METHODS

To explore the impact of biological cohesion on the dynamics of cohesive SGFs, series

CITATION: Craig, M.J., et al., 2020, Biomediation of submarine sediment gravity flow dynamics: Geology, v. 48, p. 72–76, https://doi.org/10.1130/G46837.1

of experimental SGFs were generated with and without EPS. These flows were generated in a 5-m-long, 0.2-m-wide, and 0.5-m-deep, smooth-bottomed lock-exchange tank (Fig. DR1 in the GSA Data Repository[1]). The reservoir was filled with a mixture of kaolinite clay (volumetric concentration C_{clay} = 5–23 vol%), EPS, and seawater. Xanthan gum was used as a proxy for natural EPS (cf. Tan et al., 2014). Xanthan gum shares chemical similarities with a wide variety of EPS and is widely used as a substitute for EPS in marine ecology, soil science, and sediment stability research (see the Data Repository). The range of C_{EPS} used in the experiments (0–0.268 wt%), was informed by seabed sediment cores obtained during RV *Tangaroa* cruise TAN1604, from 127 to 1872 m depths in the Hauraki Gulf, North Island of New Zealand (Figs. DR2 and DR3; Table DR1). These EPS data are based on bulk carbohydrate content, collected using the standard assay method of DuBois et al. (1956). The maximum C_{EPS} recorded in the TAN1604 cores was 0.260 wt%, with an average value of 0.139 wt%. For comparison, background EPS content ranges from 0.01 to 0.1 wt% measured in estuarine sediment and from 0.1 to 0.67 wt% measured in freshwater sediment (Gerbersdorf et al., 2009; Malarkey et al., 2015).

In the laboratory, we compared the head velocity, U_h, and runout distance of clay-only control flows with equivalent flows containing EPS to test if biological cohesion intensifies cohesive flow behavior. U_h versus horizontal distance was measured using a high-definition video camera. Flow runout distances (maximum deposit extent from the lock gate) were recorded, except for flows that traveled the length of the tank (Table 1). To examine the impact of EPS on floc dynamics, samples were extracted for floc size and density analyses, using the LabSFLOC-2 (Laboratory Spectral Flocculation Characteristics (Manning et al., 2007) method (see the Data Repository). Each flow was classified visually following Hermidas et al. (2018).

CONTROL FLOWS WITHOUT EPS

The clay-only control flows generated turbidity currents at C_{clay} = 5–15 vol% and top transitional plug flows (TTPFs; Hermidas et al., 2018) at C_{clay} = 22–23 vol%, allowing us to examine the effects of EPS in fully turbulent flows and transitional flows experiencing turbulence suppression by physical cohesion (Table 1). Turbidity currents traveled the length of the tank and generated shear waves along their upper interface with the ambient fluid (Table 2). The TTPFs featured a dense, laminar lower "plug" layer with coherent fluid entrainment structures (Baker et al., 2017; Figs. DR4 and DR5) that transitioned upward into a dilute turbulent layer (Table 2).

FLOWS WITH EPS

Adding EPS to the turbidity currents with C_{clay} < 15 vol% produced no visual changes in flow behavior and no measurable differences in the U_h profiles (Figs. DR6 and DR7). At C_{clay} = 15 vol%, the EPS-laden flows (Table 1) were also visually indistinguishable from turbulent clay-only flow F07. However, the U_h of F08 and F09 decreased more rapidly than for F07 between 4 m and 4.2 m along the tank, resulting in lower U_h values at 4.6 m (Fig. 1). At the highest C_{EPS}, F10 began to decelerate rapidly at 2.5 m and halted at 3.9 m.

TTPFs at C_{clay} = 22 vol% and C_{clay} = 23 vol% exhibited distinct decreases in U_h and runout distance as EPS were added (Fig. 2; Fig. DR8). Normalized to the maximum head velocity, $U_{h,max}$, and runout distance of the clay-only flows, the combined C_{clay} = 22 vol% and C_{clay} = 23 vol% data are strongly correlated with C_{EPS} (Figs. DR9 and DR10). In C_{clay} = 22 vol% flows, C_{EPS} ≤ 0.089 wt% still produced TTPFs

TABLE 1. BASIC EXPERIMENTAL DATA

Flow	Kaolinite C_{clay} (vol%)	EPS weight (%)	ROD (m)	$U_{h,max}$ (m s^{-1})	Flow classification
F01	5	0	–	0.377	Turbidity current
F02	5	0.134	–	0.379	Turbidity current
F03	5	0.250	–	0.381	Turbidity current
F04	10	0	–	0.367	Turbidity current
F05	10	0.132	–	0.353	Turbidity current
F06	10	0.264	–	0.348	Turbidity current
F07	15	0	–	0.430	Turbidity current
F08	15	0.066	–	0.417	Turbidity current
F09	15	0.133	–	0.416	Turbidity current
F10	15	0.265	3.91	0.420	Turbidity current
F11	22	0	4.69	0.552	TTPF
F12	22	0.067	3.63	0.455	TTPF
F13	22	0.089	3.20	0.438	TTPF
F14	22	0.133	2.13	0.217	Plug flow
F15	22	0.265	0.92	0.194	Plug flow
F16	23	0	3.66	0.471	TTPF
F17	23	0.052	2.94	0.439	TTPF
F18	23	0.087	1.80	0.419	Plug flow
F19	23	0.130	1.32	0.211	Plug flow
F20	23	0.259	0.60	0.160	Slide

Note: Flow classifications follow the scheme of Hermidas et al. (2018). C_{vol}–volumetric concentration; EPS—extracellular polymeric substances; ROD—runout distance; $U_{h,max}$—maximum head velocity; TTPF—top transitional plug flow.

TABLE 2. SUMMARY OF FLOW CLASSIFICATIONS FOLLOWING THE SCHEME OF HERMIDAS ET AL. (2018) AND CONCEPT DIAGRAMS OF FLOW BEHAVIOR AND FLOC CHARACTERISTICS

Flow Classification	Experimental Flows	Flow Diagram *(not to scale)*
Turbidity Current	F01–F10	
Top Transitional Plug Flow (TTPF)	F11-F13, F16, F17	
Plug flow	F14, F15, F18, F19	
Slump	F20	

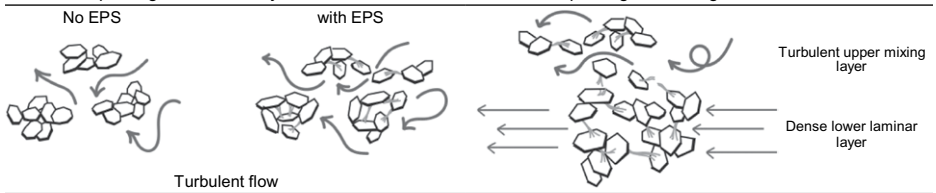

Note: EPS—extracellular polymeric substances.

[1]GSA Data Repository item 2020028, description of laboratory methods, flume tank set-up, vertical profiles of EPS concentrations and locations of TAN1604 cores, images of experimental flows, head velocity profiles of 5, 10, and 22 vol% C_{clay} flows, scatter plots of normalized run-out distances and normalized $U_{h,max}$ for 22 and 23 vol% C_{clay} flows, and scattor plot of floc size and settling velocity for 23 vol% clay-only and clay-EPS flows measured using the LabSFLOC-2 methodology, is available online at http://www.geosociety.org/datarepository/2020/, or on request from editing@geosociety.org.

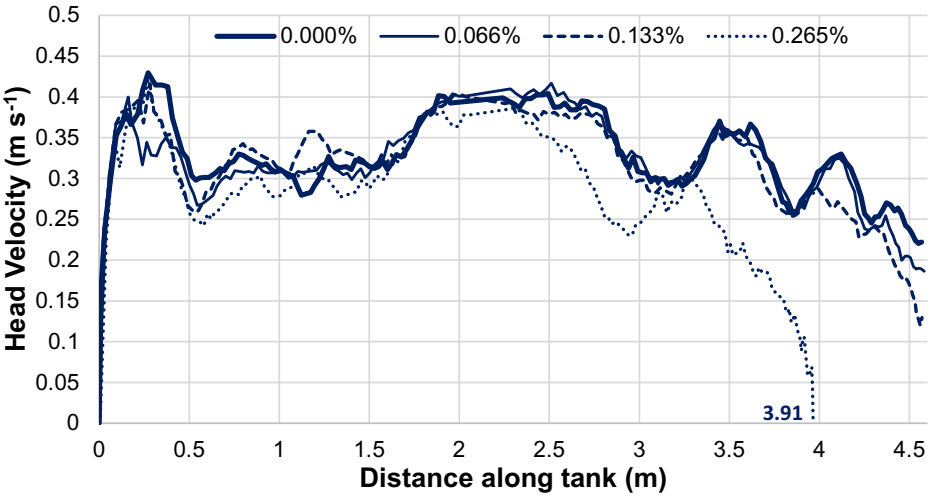

Figure 1. Head velocity of 15% kaolinite clay flows against distance traveled along the tank. Number above abscissa indicates runout distance of flow. Values in the legend correspond to extracellular polymeric substance (EPS) concentration added to the flow.

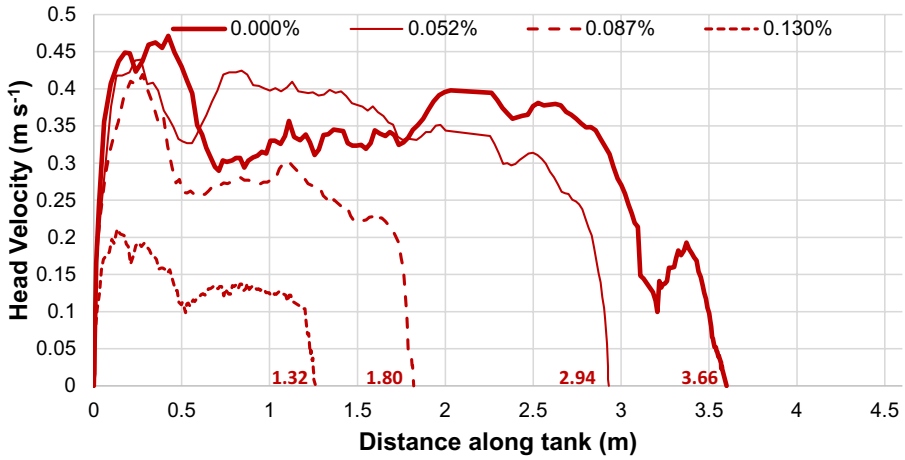

Figure 2. Head velocity of 23% kaolinite clay flows against distance traveled along the tank. Numbers above abscissa indicate runout distances of flow. Values in the legend correspond to extracellular polymeric substance (EPS) concentration added to flow.

with lower $U_{h,max}$ and shorter runout distance than the control (Fig. DR8), whereas $C_{EPS} \geq 0.133$ wt% dramatically reduced upper boundary mixing, producing a distinct interface with the ambient fluid characteristic of plug flows (Fig. DR11; Hermidas et al., 2018). Flows F14 and F15 also lacked coherent fluid entrainment structures. These flows achieved $U_{h,max}$ less than half of the $C_{clay} = 22$ vol% clay-only and clay-EPS TTPFs, and en masse freezing significantly reduced runout distance (Fig. DR8). At $C_{vol} = 23$ vol%, this change from TTPF to plug flow occurred at $C_{EPS} \geq 0.087$ wt%. At the highest C_{EPS} of 0.259 wt% in F20, the slurry slid out of the reservoir for 0.6 m (Hampton et al., 1996).

ANALYZING THE EFFECT OF EPS ON FLOW PROPERTIES

Our experiments demonstrate that the strong biological cohesion imparted by EPS in the seabed extends to SGFs at the C_{EPS} values found in deep-sea and coastal environments. U_h and runout distance were reduced by adding EPS to the TTPFs and the densest turbidity currents. At higher clay and EPS concentrations, the biological cohesion caused flow transformation, suggesting that EPS limit shear turbulence by increasing the strength of the bonds between clay flocs. These flows are likely to be non-Newtonian with a yield stress, as in aqueous xanthan gum solutions and xanthan-kaolinite mixtures (Song et al., 2006; Hamed and Belhadri, 2009). This biological cohesion was greater per unit weight than the physical cohesion. At $C_{clay} = 22$ vol%, the addition of 0.133 wt% EPS induced a flow transformation from TTPF to plug flow, substantially reducing the runout distance and $U_{h,max}$. A similar reduction in runout distance would require an increase in clay concentration from 22% to 25% in an EPS-free flow (Baker et al., 2017).

We hypothesize that EPS strengthen cohesion between flocs and assist in building a network of interconnected flocs (Leppard and Droppo, 2004). EPS in TTPFs are brought into contact with more clay particles than in turbidity currents, allowing the EPS to strengthen the particle network, further suppressing turbulence and encouraging laminar flow (Table 2).

To test this hypothesis, samples of fluid were taken from clay-only TTPF F16 and clay-EPS TTPF F17 for floc size and density comparison using LabSFLOC-2 (Fig. DR12). As each sample was released into the settling column, the gel underwent gravitational settling and broke into flocs. Only 10% of the flocs in F16 were larger than 200 µm, compared to 55% in F17. The clay-EPS flocs had a lower density than the clay-only flocs, and this difference increased up to ten times as floc size increased. The dominance of large, water-rich flocs in clay-EPS F17 implies that the clay-EPS gel was more resistant to separation into smaller flocs under shear during static settling. We further infer that within flows, these water-rich clay-EPS flocs are more resistant to shear turbulence than the clay-only flocs, and that this difference increases with increasing clay and EPS concentrations, resulting in more laminar flow behavior.

EPS IN NATURAL SEDIMENT GRAVITY FLOWS

The influence of EPS was observed in experimental turbulent, transitional, and laminar SGFs, each with complex and variable flow properties. Scaling of these flows to natural prototypes is a nontrivial task, and standard methods (e.g., Froude, Reynolds, and Shields numbers, and distorted geometric scaling) are unlikely to be valid without modification (Iverson, 1997; Marr et al., 2001; Mulder and Alexander, 2001). However, the experimental SGFs may be used as analogues for natural SGFs based on fundamental physical principles. The experimental flows traveled at <0.55 m s^{-1}; suitable analogues are hyperpycnal river discharge, and weak submarine SGFs triggered by earthquakes, which have velocities of 0.3–1.6 m s^{-1} (Talling et al., 2013), and natural SGFs that have decelerated to a similar velocity. The observed turbulence suppression is likely to apply to other flow types, such as wave- and current-driven sediment flows and fluid mud flows on shelves, which rely on turbulence to suspend particles (Traykovski et al., 2000). Turbulence modulation in higher-velocity flows, and in flows with higher turbulence intensity, is likely to occur at higher concentrations of EPS and clay than in these experiments.

IMPLICATIONS FOR THE GLOBAL CARBON CYCLE

The settling of particulate C_{org} to the seafloor is regarded as a key process in the global carbon cycle. However, measurements show that only

1%–4% of this material is buried within the seabed (Decho and Gutierrez, 2017). Large amounts of particulate C_{org} are delivered to continental shelves via rivers (0.8 PgC yr^{-1}; Liu et al., 2010) and by in situ primary production (6.2 PgC yr^{-1}; Chen, 2010). The majority is remineralized in the water column, and only a small amount is preserved on the shelf (0.2 PgC yr^{-1}; de Haas et al., 2002; Chen, 2010; Liu et al., 2010). In contrast, continental slopes are important carbon sinks. Approximately 40%–50% of C_{org} transported from the shelf to the continental slope (0.5 PgC yr^{-1}; Chen, 2010) is buried at water depths <500 m. The remaining 50%–60% is stored at >800 m (Muller-Karger et al., 2005).

The transport of C_{org} down continental slopes by SGFs has not received much attention in these calculations. However, large-scale SGFs on continental margins have the potential to move large quantities of terrestrial and marine C_{org} to the deep sea (e.g., Mountjoy et al., 2018) while also providing the rapid burial that promotes the preservation of C_{org}. The ability of EPS to alter SGF behavior, as shown here, implies that EPS change the spatial distribution of organic carbon sinks. Moreover, the increased cohesion of mixed clay-EPS flows promotes en masse deposition, which helps the burial and preservation of C_{org} by reducing oxygen exposure times (Burdige, 2007; Hedges and Keil, 1995). In the context of the global carbon cycle, a better understanding of the ability of EPS to influence the dynamics of its transport medium may improve numerical models of C_{org} fluxes on continental margins, particularly where they are dominated by fine-grained sediment input and high primary, and therefore EPS, production. Our deep-sea cores showed EPS levels similar to coastal environments, where EPS are widely recognized for their contribution to the C_{org} pool (Morelle et al., 2017). These results highlight that current global carbon budgets may underestimate C_{org} flux by not considering C_{org} transport via SGFs and the contribution of in situ EPS to the C_{org} sink in deep-sea sediment.

CONCLUDING REMARKS

Increasing numbers of studies highlight the importance of considering physical cohesion when interpreting and modeling SGF processes, but the insights into biologically cohesive SGFs presented here indicate the need to recognize the potent effects of EPS in future studies. At the concentrations found in modern estuarine, coastal, and deep-marine environments, EPS have proven to be capable of changing flow behavior and reducing the deposit runout distance and $U_{h,max}$ of cohesive flows. This research will improve our predictive models of these volumetrically significant and hazardous events. Further studies are needed to better constrain and quantify the effects of EPS in process models for cohesive and noncohesive SGFs, and their wider environmental relevance for geological history and the global carbon cycle.

ACKNOWLEDGMENTS

The Australian Government Research Training Program Scholarship funded Craig's Ph.D. candidature. An International Association of Sedimentologists Postgraduate Award Grant funded Craig's visit to Bangor University (Bangor, UK). The UK Natural Environment Research Council grant NE/1027223/1 (COHBED project) enabled this research to be undertaken using the flume facility built by Rob Evans (Bangor University). We thank Brian Scannell, Edward Lockhart, and Connor McCarron for help in the laboratory. We thank the officers, crew, and scientific complement for core collection and processing on RV *Tangaroa* cruise TAN1604, with funding via the New Zealand Strategic Science Investment Fund to the National Institute of Water & Atmospheric Research's National Centres of Coasts and Oceans and Climate, Atmosphere, and Hazards. Irvine Davidson (University of St. Andrews, UK) is thanked for his help in measuring extracellular polymeric substance concentrations in the Hauraki Gulf cores. We are also grateful for the constructive feedback from reviewers Peter Talling, Lawrence Amy, and Esther Sumner, which greatly improved this manuscript.

REFERENCES CITED

Baas, J.H., and Best, J.L., 2002, Turbulence modulation in clay-rich sediment-laden flows and some implications for sediment deposition: Journal of Sedimentary Research, v. 72, p. 336–340, https://doi.org/10.1306/120601720336.

Baas, J.H., Best, J.L., Peakall, J., and Wang, M., 2009, A phase diagram for turbulent, transitional, and laminar clay suspension flows: Journal of Sedimentary Research, v. 79, p. 162–183, https://doi.org/10.2110/jsr.2009.025.

Baker, M.L., Baas, J.H., Malarkey, J., Jacinto, R.S., Craig, M.J., Kane, I.A., and Barker, S., 2017, The effect of clay type on the properties of cohesive sediment gravity flows and their deposits: Journal of Sedimentary Research, v. 87, p. 1176–1195, https://doi.org/10.2110/jsr.2017.63.

Barker, S.P., Haughton, P.D., McCaffrey, W.D., Archer, S.G., and Hakes, B., 2008, Development of rheological heterogeneity in clay-rich high-density turbidity currents: Aptian Britannia Sandstone Member, UK continental shelf: Journal of Sedimentary Research, v. 78, p. 45–68, https://doi.org/10.2110/jsr.2008.014.

Burdige, D.J., 2007, Preservation of organic matter in marine sediments: Controls, mechanisms, and an imbalance in sediment organic carbon budgets?: Chemical Reviews, v. 107, p. 467–485, https://doi.org/10.1021/cr050347q.

Chen, C.-T.A., 2010, Cross-boundary exchanges of carbon and nitrogen in continental margins, *in* Liu, K.K., et al., eds., Carbon and Nutrient Fluxes in Continental Margins: Berlin, Springer, p. 561–574, https://doi.org/10.1007/978-3-540-92735-8_13.

Decho, A.W., and Gutierrez, T., 2017, Microbial extracellular polymeric substances (EPSs) in ocean systems: Frontiers in Microbiology, v. 8, p. 922, https://doi.org/10.3389/fmicb.2017.00922.

de Haas, H., van Weering, T.C., and de Stigter, H., 2002, Organic carbon in shelf seas: Sinks or sources, processes and products: Continental Shelf Research, v. 22, p. 691–717, https://doi.org/10.1016/S0278-4343(01)00093-0.

DuBois, M., Gilles, K.A., Hamilton, J.K., Rebers, P.T., and Smith, F., 1956, Colorimetric method for determination of sugars and related substances: Analytical Chemistry, v. 28, p. 350–356, https://doi.org/10.1021/ac60111a017.

Falkowski, P.G., Barber, R.T., and Smetacek, V., 1998, Biogeochemical controls and feedbacks on ocean primary production: Science, v. 281, p. 200–206, https://doi.org/10.1126/science.281.5374.200.

Galy, V., France-Lanord, C., Beyssac, O., Faure, P., Kudrass, H., and Palhol, F., 2007, Efficient organic carbon burial in the Bengal Fan sustained by the Himalayan erosional system: Nature, v. 450, p. 407–410, https://doi.org/10.1038/nature06273.

Gerbersdorf, S.U., Westrich, B., and Paterson, D.M., 2009, Microbial extracellular polymeric substances (EPS) in fresh water sediments: Microbial Ecology, v. 58, p. 334–349, https://doi.org/10.1007/s00248-009-9498-8.

Hamed, S.B., and Belhadri, M., 2009, Rheological properties of biopolymers drilling fluids: Journal of Petroleum Science Engineering, v. 67, p. 84–90, https://doi.org/10.1016/j.petrol.2009.04.001.

Hampton, M.A., Lee, H.J., and Locat, J., 1996, Submarine landslides: Reviews of Geophysics, v. 34, p. 33–59, https://doi.org/10.1029/95RG03287.

Hedges, J.I., and Keil, R.G., 1995, Sedimentary organic matter preservation: An assessment and speculative synthesis: Marine Chemistry, v. 49, p. 81–115, https://doi.org/10.1016/0304-4203(95)00008-F.

Hermidas, N., Eggenhuisen, J.T., Jacinto, R.S., Luthi, S.M., Toth, F., and Pohl, F., 2018, A classification of clay-rich subaqueous density flow structures: Journal of Geophysical Research–Earth Surface, v. 123, p. 945–966, https://doi.org/10.1002/2017JF004386.

Hillier, S., 1995, Erosion, sedimentation and sedimentary origin of clays, *in* Veld, B., ed., Origin and Mineralogy of Clays: Berlin, Springer-Verlag, p. 162–219, https://doi.org/10.1007/978-3-662-12648-6_4.

Iverson, R.M., 1997, The physics of debris flows: Reviews of Geophysics, v. 35, p. 245–296, https://doi.org/10.1029/97RG00426.

Leppard, G.G., and Droppo, I.G., 2004, Overview of flocculation processes in freshwater ecosystems, *in* Droppo, I.G., et al., eds., Flocculation in Natural and Engineered Environmental Systems: Boca Raton, Florida, CRC Press, p. 25–46, https://doi.org/10.1201/9780203485330.pt1.

Liu, K.-K., Atkinson, L., Quiñones, R.A., and Talaue-McManus, L., 2010, Biogeochemistry of continental margins in a global context, *in* Liu, K.-K., et al., eds., Carbon and Nutrient Fluxes in Continental Margins: Berlin, Springer-Verlag, p. 3–24, https://doi.org/10.1007/978-3-540-92735-8_1.

Malarkey, J., et al., 2015, The pervasive role of biological cohesion in bedform development: Nature Communications, v. 6, p. 6257, https://doi.org/10.1038/ncomms7257.

Manning, A.J., Friend, P.L., Prowse, N., and Amos, C.L., 2007, Estuarine mud flocculation properties determined using an annular mini-flume and the LabSFLOC system: Continental Shelf Research, v. 27, p.1080–1095, https://doi.org/10.1016/j.csr.2006.04.011.

Marr, J.G., Harff, P.A., Shanmugam, G., and Parker, G., 2001, Experiments on subaqueous sandy gravity flows: The role of clay and water content in flow dynamics and depositional structures: Geological Society of America Bulletin, v. 113, p. 1377–1386, https://doi.org/10.1130/0016-7606(2001)113<1377:EOSSGF>2.0.CO;2.

Martin, J.H., Knauer, G.A., Karl, D.M., and Broenkow, W.W., 1987, VERTEX: Carbon cycling in the northeast Pacific: Deep-Sea Research, Part A, Oceanographic Research Papers, v. 34, p. 267–285, https://doi.org/10.1016/0198-0149(87)90086-0.

McCave, I., and Jones, K., 1988, Deposition of ungraded muds from high-density non-turbulent turbidity currents: Nature, v. 333, p. 250–252, https://doi.org/10.1038/333250a0.

Morelle, J., Schapira, M., and Claquin, P., 2017, Dynamics of phytoplankton productivity and exopolysaccharides (EPS and TEP) pools in the Seine Estuary (France, Normandy) over tidal cycles and over two contrasting seasons: Marine Environmental Research, v. 131, p. 162–176, https://doi.org/10.1016/j.marenvres.2017.09.007.

Mountjoy, J.J., Howarth, J.D., Orpin, A.R., Barnes, P.M., Bowden, D.A., Rowden, A.A., Schimel, A.C., Holden, C., Horgan, H.J., and Nodder, S.D., 2018, Earthquakes drive large-scale submarine canyon development and sediment supply to deep-ocean basins: Science Advances, v. 4, p. eaar3748, https://doi.org/0.1126/sciadv.aar3748.

Mulder, T., and Alexander, J., 2001, The physical character of subaqueous sedimentary density flows and their deposits: Sedimentology, v. 48, p. 269–299, https://doi.org/10.1046/j.1365-3091.2001.00360.x.

Muller-Karger, F.E., Varela, R., Thunell, R., Luerssen, R., Hu, C., and Walsh, J.J., 2005, The importance of continental margins in the global carbon cycle: Geophysical Research Letters, v. 32, L01602, https://doi.org/10.1029/2004GL021346.

Song, K.-W., Kim, Y.-S., and Chang, G.-S., 2006, Rheology of concentrated xanthan gum solutions: Steady shear flow behavior: Fibers and Polymers, v. 7, p. 129–138, https://doi.org/10.1007/BF02908257.

Sumner, E.J., Talling, P.J., and Amy, L.A., 2009, Deposits of flows transitional between turbidity current and debris flow: Geology, v. 37, p. 991–994, https://doi.org/10.1130/G30059A.1.

Talling, P.J., 2014, On the triggers, resulting flow types and frequencies of subaqueous sediment density flows in different settings: Marine Geology, v. 352, p. 155–182, https://doi.org/10.1016/j.margeo.2014.02.006.

Talling, P.J., Paull, C.K., and Piper, D.J., 2013, How are subaqueous sediment density flows triggered, what is their internal structure and how does it evolve? Direct observations from monitoring of active flows: Earth-Science Reviews, v. 125, p. 244–287, https://doi.org/10.1016/j.earscirev.2013.07.005.

Tan, X., Hu, L., Reed, A.H., Furukawa, Y., and Zhang, G., 2014, Flocculation and particle size analysis of expansive clay sediments affected by biological, chemical, and hydrodynamic factors: Ocean Dynamics, v. 64, p. 143–157, https://doi.org/10.1007/s10236-013-0664-7.

Tolhurst, T., Gust, G., and Paterson, D., 2002, The influence of an extracellular polymeric substance (EPS) on cohesive sediment stability: Proceedings in Marine Science, v. 5, p. 409–425, https://doi.org/10.1016/S1568-2692(02)80030-4.

Traykovski, P., Geyer, W.R., Irish, J., and Lynch, J., 2000, The role of wave-induced density-driven fluid mud flows for cross-shelf transport on the Eel River continental shelf: Continental Shelf Research, v. 20, p. 2113–2140, https://doi.org/10.1016/S0278-4343(00)00071-6.

Wright, L., and Friedrichs, C., 2006, Gravity-driven sediment transport on continental shelves: A status report: Continental Shelf Research, v. 26, p. 2092–2107, https://doi.org/10.1016/j.csr.2006.07.008.

Printed in USA